2016 American Control Conference (ACC)
Boston Marriott Copley Place
July 6-8, 2016. Boston, MA, USA

Bayesian Occupancy Grid Mapping via an Exact Inverse Sensor Model

Evan Kaufman, Taeyoung Lee, Zhuming Ai, and Ira S. Moskowitz

Abstract— **Occupancy grid maps are spatial representations of environments, where the space of interest is decomposed into a number of cells that are considered either occupied or free. This paper focuses on occupancy grid mapping, which is to estimate the probability of occupancy for each cell based on range measurements from a known location. For a given probabilistic model of a range sensor, we propose a computationally efficient method to obtain an exact inverse sensor model, and it is utilized to construct a probabilistic mapping algorithm according to the Bayesian framework. Compared with the existing occupancy grid mapping techniques that rely on approximate, heuristic inverse sensor models, the proposed approach yields substantially more accurate maps for the same set of measurements. These are illustrated by numerical examples and experiments.**

I. Introduction

Robotic mapping is the process of generating maps, which represent the environment in close proximity of a robot. This problem is crucial to understanding the surrounding regions when a robot enters an uncertain environment. Various map representations include occupancy grids [1], octomaps [2], or feature-based maps [3].

This paper focusses on the popular occupancy grid representation, where the map space is decomposed into evenly-spaced grid cells, considered as either occupied or free. The *inverse sensor model* is the probability of occupancy for a grid cell based on range measurements and the configuration of the mobile robot, which is of fundamental importance with occupancy grid mapping. However, the exact solution to the inverse sensor model has not been utilized in occupancy grid mapping, because the computational requirements are too cumbersome to compute the exact model in real time [4].

Instead, several techniques have been proposed to approximate the exact inverse sensor model. In the early occupancy grid mapping applications based on sonar sensors, *ad hoc* techniques to obtain an inverse sensor model were developed based off highly-innacurate bouncing sound waves [5], [6]. These techniques are based on approximate functions to represent the inverse sensor model with questionable accuracy [7] and applied to more modern sensors in [8], [9].

The other popular approach to obtain an approximate inverse sensor model is to simulate maps, robot poses, and measurements and use a learning algorithm to approximate the inverse sensor model [4], [10]. These approaches are undesirable in practice due to complexities associated to implementing a learning algorithm. For example, the accuracy of such inverse sensor models strongly depends on the samples selected for learning, but it is unclear how to select those samples, or how many samples are required to obtain a reasonable approximation. Furthermore, it is challenging to apply any learning algorithm over the large dimensional space composed of maps, poses, and measurements.

This paper proposes a computationally efficient algorithm to construct the exact inverse sensor model. More explicitly, for a given forward sensor model defined by the probability distribution of range measurements, this algorithm yields the a posteriori probability of occupancy of all the cells within the area covered by the range sensor from the range measurements. The key idea is reducing the computational load by using the fact that if a cell is occupied, the occupancy of the other cells blocked by it is irrelevant to the forward sensor model, and this model is systematically utilized with various probabilistic properties to derive a computationally-efficient solution to the inverse sensor model. Furthermore, the proposed approach integrates a priori probability of occupancy and multiple range measurements according to the Bayesian framework to obtain more accurate maps. As such, it contrasts from the existing framework based on log-odds ratios that impose an additional Markov assumption.

In short, the main contribution of this paper is proposing the exact inverse sensor model and constructing a Bayesian occupancy grid mapping based on that. Compared with the current mapping algorithms based on an approximate inverse sensor model, this approach yields more accurate occupancy probabilities. This constructs substantially more accurate occupancy grid maps with less uncertainty for the same set of measurements, and these are directly illustrated by numerical examples and preliminary experimental results. While this paper is focused on the mapping problem in two-dimensional environments, the presented results can be certainly utilized in SLAM or stochastic motion planning in three dimensions.

II. Problem Formulation

A. Range Sensor

Consider a range sensor that provides scans of the surrounding environment in order to identify the closest occupied space. The location and the direction of the sensor, referred to as the *pose* at time t, is denoted by X_t. The range sensor returns a measurement *scan* Z_t, composed of n_z measurement *rays* $z_{t,1}, z_{t,2}, \ldots, z_{t,n_z}$. The l-th measurement ray for $l \in \{1, 2, \ldots, n_z\}$ contains the depth (range) and bearing (direction) inside the sensor field of view (FOV) that

Evan Kaufman, Taeyoung Lee, Mechanical and Aerospace Engineering, George Washington University, Washington DC 20052 {evankaufman,tylee}@gwu.edu

Zhuming Ai, Ira S. Moskowitz, Information Management & Decision Architectures, U.S. Naval Research Laboratory, Washington, DC 20375

This research has been supported by the U.S. Naval Research Laboratory Base Program Work Unit "Intelligent Microflyer" and in part by NSF under the grants CMMI-1243000, CMMI-1335008, and CNS-1337722.

corresponds to a circular sector. Given X_t, we assume the origin and directions of each ray are known deterministically.

The probability density function, namely $p(z_{t,l}|m, X_t)$ with respect to the depth of the l-th measurement ray conditioned on the map m and the pose X_t is commonly referred to as the *forward sensor model*, which characterizes the corresponding depth sensor, such as the maximum range or accuracy. The forward sensor model satisfies (i) the ranges of all depth measurements are positive and finite, and (ii) measurement rays cannot pass through occupied regions.

Throughout this paper, we assume that the forward sensor model of the selected sensor is given. This can be determined empirically or analytically. For example, the *beam model for range finders* satisfying the above criteria is described in [4].

B. Occupancy Grid Mapping

Let a map m be decomposed into n_m evenly-spaced grid cells, where the i-th grid cell is assigned to a static binary random variable $\mathbf{m}_i$ for $i \in \{1, 2, \ldots, n_m\}$, that is defined as $\mathbf{m}_i = 1$ when occupied, and $\mathbf{m}_i = 0$ when free. The location and size of each grid cell is assumed known. Therefore, a map m is defined by $\{\mathbf{m}_1, \ldots, \mathbf{m}_{n_m}\}$ (2^{n_m} possible maps).

Another random variable is defined as $\bar{\mathbf{m}}_i = 1 - \mathbf{m}_i$ for convenience. The probability that the i-th cell is occupied is $P(\mathbf{m}_i)$, and the probability that it is free is $P(\bar{\mathbf{m}}_i) = 1 - P(\mathbf{m}_i)$. The random variables $\mathbf{m}_i$ are mutually independent,

$$P(m) = P(\mathbf{m}_1, \mathbf{m}_2, \ldots, \mathbf{m}_{n_m}) = \prod_{i=1}^{n_m} P(\mathbf{m}_i). \quad (1)$$

Occupancy grid mapping is to determine these probabilities based on robot poses and measurement scans. More explicitly, let $X_{1:t}$ denote the history of poses from the initial time to the current time, $\{X_1, X_2, \ldots, X_t\}$, and let $Z_{1:t}$ be the measurement history. The goal is to obtain $P(\mathbf{m}_i|X_{1:t}, Z_{1:t})$, commonly referred to as the *inverse sensor model* for given forward sensor model $p(z_{t,l}|m, X_t)$ and the initial estimate of the map $P(m)$ with $X_{1:t}$ and $Z_{1:t}$.

C. Mapping via Log-Odds Ratio

One of the popular frameworks of updating binary random variables with static state is with a binary Bayesian filter using the log-odds ratio formulation. The main idea is that instead of multiplying terms from prior and current time steps, the properties of logarithms allow these terms to be simply added, while avoiding truncation issues associated with probabilities close to 0 or 1 [4]. The log-odds ratio is also popular because learning techniques with forward models [10], [11] or ad hoc techniques [5], [6] are simpler to derive when they need not consider $P(\mathbf{m}_i|X_{1:t}, Z_{1:t-1})$ as part of the inverse sensor model, but rather only $P(\mathbf{m}_i)$, which is typically fixed and uniform for all cells.

However, the log-odds ratio formulation makes an assumption that is not consistent with the occupancy grid mapping problem. It is assumed that if X_t and $\mathbf{m}_i$ are known, then Z_t is independent of $X_{1:t-1}$ and $Z_{1:t-1}$, i.e.,

$$P(Z_t|\mathbf{m}_i, X_{1:t}, Z_{1:t-1}) \approx P(Z_t|\mathbf{m}_i, X_t). \quad (2)$$

However, forward models are based on the entire map m. Since (2) conditioned only by the i-th cell, past poses $X_{1:t-1}$ and past measurement scans $Z_{1:t-1}$ may contain important information about the occupancy of the other cells, which should be considered in calculating the probability distribution of the measurement scan Z_t.

III. Exact Inverse Sensor Model

Due to computational complexity, approximate inverse sensor models have been used for occupancy grid mapping with simplifying assumptions. In this section, we propose an algorithm to compute the exact inverse sensor model efficiently. We present two versions according to Bayesian framework. The first type is referred to as the *ray inverse sensor model* $P(\mathbf{m}_i|X_{1:t}, Z_{1:t-1}, z_{t,l})$, which only considers l-th ray at time t, i.e., one-dimensional inverse sensor model. The second type is referred to as the *scan inverse sensor model* $P(\mathbf{m}_i|X_{1:t}, Z_{1:t})$, which combines the information from *all* measurement rays *simultaneously* at the t-th time step for two-dimensional cases. These are developed in a sequential form to be repeated at each time step.

A. Ray Inverse Sensor Model

Suppose the probability of the map conditioned on the past poses and measurements, namely $P(m|X_{1:t-1}, Z_{1:t-1})$, is known. Here we construct a posteriori probability $P(m|z_{t,l}, X_{1:t}, Z_{1:t-1})$, based on the current pose X_t, the measurement from the l-th ray $z_{t,l}$, and the given forward sensor model $p(z_{t_l}|m, X_t)$.

a) Bayesian Framework: Bayes' rule yields

$$P(m|z_{t,l}, X_{1:t}, Z_{1:t-1}) = \frac{p(z_{t,l}|m, X_{1:t}, Z_{1:t-1})P(m|X_{1:t-1}, Z_{1:t-1})}{p(z_{t,l}|X_{1:t}, Z_{1:t-1})}, \quad (3)$$

considering that X_t carries no information about m without Z_t. If the current pose X_t and map m are known, then the measurement ray $z_{t,l}$ is independent of past poses $X_{1:t-1}$ and past measurements $Z_{1:t-1}$ to obtain

$$P(m|z_{t,l}, X_{1:t}, Z_{1:t-1}) = \eta_{t,l} p(z_{t,l}|m, X_t) P(m|X_{1:t-1}, Z_{1:t-1}), \quad (4)$$

where the normalizing constant $\eta_{t,l} \in \mathbb{R}$ absorbs all terms independent of the map m.

Next, we compute the occupancy probability of each cell. Let $\mathcal{M}_i$ be the set of maps where the i-th cell is occupied, i.e., $\mathcal{M}_i = \{m \in \{0,1\}^{n_m} \mid \mathbf{m}_i = 1\}$. To compute the probability of occupancy of the i-th cell, all possible combinations of map in $\mathcal{M}_i$ should be considered, i.e.,

$$P(\mathbf{m}_i|z_{t,l}, X_{1:t}, Z_{1:t-1}) = \eta_{t,l} \sum_{m \in \mathcal{M}_i} p(z_{t,l}|m, X_t) P(m|X_{1:t-1}, Z_{1:t-1}). \quad (5)$$

Furthermore, to determine the normalizing constant $\eta_{t,l}$, the complement $P(\bar{\mathbf{m}}_i|z_{t,l}, X_{1:t}, Z_{1:t-1})$ must be calculated in the similar manner. Since there are 2^{n_m-1} maps in $\mathcal{M}_i$, these equations require 2^{n_m} terms to compute the summation for

the i-th grid cell, and it should be repeated for other cells. This is the main reason why the current results are based on certain approximations of the above expression.

b) Computationally Efficient Approach: We propose a computational algorithm to evaluate (5) efficiently. Since the cells outside of the sensor FOV are not affected, we focus on a reduced map r_l in the FOV of the l-th ray. This reduced map is chosen such that each cell of r_l corresponds to a grid cell of m that the l-th ray intersects, ordered by increasing distance, which is easily determined from geometry. Let $\mathbf{r}_{l,k}$ be the binary random variable representing the occupancy of the k-th cell of the l-th ray. The number of cells in the reduced map is denoted by $n_{r,l} \leq n_m$.

Next, let $\mathbf{r}_{l,k+}$ correspond to the set of maps that the k-th cell of the l-th ray is occupied, cells with lower index are free, and cells with greater index may or may not be occupied. In other words, the k-th cell $\mathbf{r}_{l,k}$ is the closest occupied cell to current pose X_t along the l-th ray. Then, the forward sensor model is identical for all maps defined by $\mathbf{r}_{l,k+}$, regardless of the occupancy of the cells beyond the k-th cell, and the corresponding forward sensor model $p(z_{t,l}|\mathbf{r}_{l,k+}, X_t)$ depends on the distance from X_t to the k-th cell. Based on this, we present the following computational algorithm to compute the inverse sensor model.

Proposition 1 *For the l-th measurement ray, the a posteriori probability of the occupancy of the k-th cell, namely the ray inverse sensor model is given by*

$$P(\mathbf{r}_{l,k}|z_{t,l}, X_{1:t}, Z_{1:t-1}) = \eta_{t,l}\tilde{P}(\mathbf{r}_{l,k}|z_{t,l}, X_{1:t}, Z_{1:t-1}), \tag{6}$$

where the unnormalized probability of the inverse sensor model is defined as

$$\begin{aligned}
&\tilde{P}(\mathbf{r}_{l,k}|z_{t,l}, X_{1:t}, Z_{1:t-1}) \\
&= P(\mathbf{r}_{l,k}|X_{1:t-1}, Z_{1:t-1}) \\
&\quad \times \left[\sum_{i=1}^{k-1} \left\{ \prod_{j=0}^{i-1} P(\bar{\mathbf{r}}_{l,j}|X_{1:t-1}, Z_{1:t-1}) \right\} \right. \\
&\quad \left. \times\, p(z_{t,l}|\mathbf{r}_{l,i+}, X_t) P(\mathbf{r}_{l,i}|X_{1:t-1}, Z_{1:t-1}) \right] \\
&\quad + \left\{ \prod_{j=0}^{k-1} P(\bar{\mathbf{r}}_{l,j}|X_{1:t-1}, Z_{1:t-1}) \right\} \\
&\quad \times\, p(z_{t,l}|\mathbf{r}_{l,k+}, X_t) P(\mathbf{r}_{l,k}|X_{1:t-1}, Z_{1:t-1}),
\end{aligned} \tag{7}$$

where $P(\bar{\mathbf{r}}_{l,0}|X_{1:t-1}, Z_{1:t-1}) = P(\mathbf{r}_{l,n_r+1}|X_{1:t-1}, Z_{1:t-1}) = 1$ is chosen for convenience and $p(z_{t,l}|\mathbf{r}_{l,(n_r+1)+}, X_t)$ represents the forward sensor model of a maximum sensor reading. The normalizer $\eta_{t,l}$ is given by

$$\begin{aligned}
\eta_{t,l} = \Bigg[&\sum_{i=1}^{n_{r,l}+1} \left\{ \prod_{j=0}^{i-1} P(\bar{\mathbf{r}}_{l,j}|X_{1:t-1}, Z_{1:t-1}) \right\} \\
&\times\, p(z_{t,l}|\mathbf{r}_{l,i+}, X_t) P(\mathbf{r}_{l,i}|X_{1:t-1}, Z_{1:t-1}) \Bigg]^{-1},
\end{aligned} \tag{8}$$

and it is independent of the cell index k.

Proof: See Appendix A. ∎

Note that the a priori estimate, $P(\mathbf{r}_{l,k}|X_{1:t-1}, Z_{1:t-1})$ and its compliment $P(\bar{\mathbf{r}}_{l,k}|X_{1:t-1}, Z_{1:t-1}) = 1 - P(\mathbf{r}_{l,k}|X_{1:t-1}, Z_{1:t-1})$ are available at the t-th step. Then, (6) yields a sequential occupancy grid mapping that can be applied whenever new measurements are available.

Compared with (5), where the terms of the summation should be repeated $2^{n_{r,l}}$ times *per each cell of the reduced map*, the proposed expressions (6) and (8) are *substantially* simpler as they require k summation terms for the k-th cell. In fact, if (7) and (8) are obtained recursively, requiring $O(n_{r,l}+1)$ rather than $O(n_{r,l} \times 2^{n_{r,l}})$ time as previously thought for *all cells of the reduced map*, this yields an algorithm that is $\mathbf{n_{r,l}} \times \mathbf{2^{n_{r,l}}}/(\mathbf{n_{r,l}}+\mathbf{1})$ **times faster**.

B. Scan Inverse Sensor Model

The above one-dimensional ray inverse sensor model may be generalized into a two-dimensional scan inverse sensor model by updating the map sequentially for each ray, according to

$$\begin{aligned}
&P(\mathbf{m}_i|X_{1:t}, Z_{1:t}) \\
&\quad = P((\ldots(((\mathbf{m}_i|X_{1:t}, Z_{1:t-1})|z_{t,1})|z_{t,2})|\ldots)|z_{t,n_z}).
\end{aligned} \tag{9}$$

Alternatively, measurements from multiple rays can be integrated synergistically, based on the assumption that the measurements of rays are mutually independent, i.e., $p(z_{t,1}, z_{t,2}, \ldots, z_{t,n_z}|\mathbf{m}_i, X_{1:t}, Z_{1:t-1}) = \prod_{l=1}^{n_z} p(z_{t,l}|\mathbf{m}_i, X_{1:t}, Z_{1:t-1})$. Let $\mathcal{L}_i \subset \{1, \ldots, n_z\}$ be the set of rays intersecting the i-th cell, $\mathbf{m}_i$. Applying Bayes' rule repeatedly, we obtain

$$\begin{aligned}
&P(\mathbf{m}_i|X_{1:t}, Z_{1:t}) \\
&= \tilde{\zeta}_i \left\{ \prod_{l \in \mathcal{L}_i} p(z_{t,l}|\mathbf{m}_i, X_{1:t}, Z_{1:t-1}) \right\} P(\mathbf{m}_i|X_{1:t-1}, Z_{1:t-1}) \\
&= \zeta_i P(\mathbf{m}_i|X_{1:t-1}, Z_{1:t-1}) \prod_{l \in \mathcal{L}_i} \frac{P(\mathbf{m}_i|z_{t,l}, X_{1:t}, Z_{1:t-1})}{P(\mathbf{m}_i|X_{1:t-1}, Z_{1:t-1})},
\end{aligned} \tag{10}$$

where $\tilde{\zeta}_i, \zeta_i \in \mathbb{R}$ correspond to normalizing constants.

Suppose the l-th measurement ray intersects with the cell $\mathbf{m}_i$, where $\mathbf{r}_{l,k}$ corresponds to the cell $\mathbf{m}_i$ in the l-th reduced map, so $\mathbf{r}_{l,k} = \mathbf{m}_i$. Then, we have $P(\mathbf{m}_i|z_{t,l}, X_{1:t}, Z_{1:t-1}) = P(\mathbf{r}_{l,k}|z_{t,l}, X_{1:t}, Z_{1:t-1}) = \eta_{t,l}\tilde{P}(\mathbf{r}_{l,k}|z_{t,l}, X_{1:t}, Z_{1:t-1})$. Using this, (10) is rewritten as

$$\begin{aligned}
P(\mathbf{m}_i|X_{1:t}, Z_{1:t}) = \xi_i P(\mathbf{m}_i|X_{1:t-1}, Z_{1:t-1}) \\
\times \prod_{l \in \mathcal{L}_i} \hat{P}(\mathbf{r}_{l,k}|z_{t,l}, X_{1:t}, Z_{1:t-1}),
\end{aligned} \tag{11}$$

where the normalizer ξ_i is composed of the product of normalizers ζ_i, and η_i. Here, we introduce a new term $\hat{P}(\mathbf{r}_{l,k}|z_{t,l}, X_{1:t}, Z_{1:t-1})$ for computational efficiency as

$$\begin{aligned}
&\hat{P}(\mathbf{r}_{l,k}|z_{t,l}, X_{1:t}, Z_{1:t-1}) \triangleq \frac{\tilde{P}(\mathbf{r}_{l,k}|z_{t,l}, X_{1:t}, Z_{1:t-1})}{P(\mathbf{m}_i|X_{1:t-1}, Z_{1:t-1})} \\
&= \sum_{i=1}^{k-1} \left\{ \prod_{j=0}^{i-1} P(\bar{\mathbf{r}}_{l,j}|X_{1:t-1}, Z_{1:t-1}) \right\}
\end{aligned}$$

$$\times p(z_{t,l}|\mathbf{r}_{l,i+}, X_t)P(\mathbf{r}_{l,i}|X_{1:t-1}, Z_{1:t-1}) + \left\{\prod_{j=0}^{k-1} P(\bar{\mathbf{r}}_{l,j}|X_{1:t-1}, Z_{1:t-1})\right\} p(z_{t,l}|\mathbf{r}_{l,k+}, X_t), \quad (12)$$

where we have used (7). Similarly, its complement is

$$P(\bar{\mathbf{m}}_i|X_{1:t}, Z_{1:t}) = \xi_i P(\bar{\mathbf{m}}_i|X_{1:t-1}, Z_{1:t-1}) \times \prod_{l\in\mathcal{L}_i} \hat{P}(\bar{\mathbf{r}}_{l,k}|z_{t,l}, X_{1:t}, Z_{1:t-1}), \quad (13)$$

where $\hat{P}(\bar{\mathbf{r}}_{l,k}|z_{t,l}, X_{1:t}, Z_{1:t-1})$ is defined as

$$\begin{aligned}\hat{P}(\bar{\mathbf{r}}_{l,k}|z_{t,l}, X_{1:t}, Z_{1:t-1}) &\triangleq \frac{\tilde{P}(\bar{\mathbf{r}}_{l,k}|z_{t,l}, X_{1:t}, Z_{1:t-1})}{P(\bar{\mathbf{m}}_i|X_{1:t}, Z_{1:t-1})} \\ &= \sum_{i=1}^{k-1}\left\{\prod_{j=0}^{i-1} P(\bar{\mathbf{r}}_{l,j}|X_{1:t-1}, Z_{1:t-1})\right\} \\ &\quad \times p(z_{t,l}|\mathbf{r}_{l,i+}, X_t)P(\mathbf{r}_{l,i}|X_{1:t-1}, Z_{1:t-1}) \\ &\quad + \sum_{i=k+1}^{n_{r,l}+1}\left\{\prod_{j=0, j\neq k}^{i-1} P(\bar{\mathbf{r}}_{l,j}|X_{1:t-1}, Z_{1:t-1})\right\} \\ &\quad \times p(z_{t,l}|\mathbf{r}_{l,i+}, X_t)P(\mathbf{r}_{l,i}|X_{1:t-1}, Z_{1:t-1}), \end{aligned} \quad (14)$$

which is obtained from (24). Since

$$P(\mathbf{m}_i|X_{1:t}, Z_{1:t}) + P(\bar{\mathbf{m}}_i|X_{1:t}, Z_{1:t}) = 1,$$

the normalizer ξ_i is obtained using (11) and (13) as,

$$\xi_i = \left[P(\mathbf{m}_i|X_{1:t-1}, Z_{1:t-1}) \prod_{\mathcal{L}_i} \hat{P}(\mathbf{r}_{l,k}|z_{t,l}, X_{1:t}, Z_{1:t-1}) + P(\bar{\mathbf{m}}_i|X_{1:t-1}, Z_{1:t-1}) \prod_{\mathcal{L}_i} \hat{P}(\bar{\mathbf{r}}_{l,k}|z_{t,l}, X_{1:t}, Z_{1:t-1})\right]^{-1}, \quad (15)$$

which is substituted into (11) to obtain $P(\mathbf{m}_i|X_{1:t}, Z_{1:t})$.

C. Summary of Algorithm

In short, the proposed scan inverse sensor model is computed by (11)-(15). These are summarized in Table I as a computationally efficient, recursive algorithm that avoids several repeated calculations of the same quantity. This algorithm utilizes the following temporary variables to develop the algorithm in an efficient recursive form,

$$\begin{aligned} a_k &= \sum_{i=1}^{k-1}\left\{\prod_{j=0}^{i-1} P(\bar{\mathbf{r}}_{l,j}|X_{1:t-1}, Z_{1:t-1})\right\} \\ &\quad \times p(z_{t,l}|\mathbf{r}_{l,i}, X_t)P(\mathbf{r}_{l,i}|X_{1:t-1}, Z_{1:t-1}), \\ b_k &= \prod_{j=0}^{k-1} P(\bar{\mathbf{r}}_{l,j}|X_{1:t-1}, Z_{1:t-1}), \\ c_k &= \sum_{i=k+1}^{n_{r,l}+1}\left\{\prod_{j=0, j\neq k}^{i-1} P(\bar{\mathbf{r}}_{l,j}|X_{1:t-1}, Z_{1:t-1})\right\} \\ &\quad \times p(z_{t,l}|\mathbf{r}_{l,i+}, X_t)P(\mathbf{r}_{l,i}|X_{1:t-1}, Z_{1:t-1}). \end{aligned}$$

In contrast to the current approximate inverse sensor models, the proposed algorithm evaluates the exact inverse sensor model (5) efficiently without relying on assumptions like (2), while integrating multiple measurements synergistically. Therefore, it yields substantially more accurate maps for the same set of measurements. These are illustrated by numerical examples and experiments as follows.

```
for l = 1, 2, ..., n_z
  Obtain reduced map r_{t,l}
  Define P(r_{l,0}|X_{1:t-1}, Z_{1:t-1}) = 0, P(r̄_{l,0}|X_{1:t-1}, Z_{1:t-1}) = 1,
         P(r_{l,n_r+1}|X_{1:t-1}, Z_{1:t-1}) = 1;
  for k = 1, 2, ..., n_r
    Obtain p(z_{t,l}|X_t, r_{l,k}) from a forward sensor model
    if k = 1
      a_1 = 0, b_1 = 1;
    else
      a_k = a_{k-1} + b_{k-1} p(z_{t,l}|r_{l,k-1}, X_t) P(r_{l,k-1}|X_{1:t-1}, Z_{1:t-1});
      b_k = b_{k-1} P(r̄_{l,k-1}|X_{1:t-1}, Z_{1:t-1});
    end if
  end for
  c_{n_{r,l}+1} = 0;
  for k = n_{r,l}, n_{r,l} - 1, ..., 1
    c_k = P(r_{l,k+1}|X_{1:t-1}, Z_{1:t-1}) / P(r̄_{l,k}|X_{1:t-1}, Z_{1:t-1}) c_{k+1}
          + b_k p(z_{t,l}|r_{l,k+1}, X_t) P(r_{l,k+1}|X_{1:t-1}, Z_{1:t-1});
  end for
  for k = 1, 2, ..., n_r
    P̂(r_{l,k}|z_{t,l}, X_{1:t}, Z_{1:t-1}) = a_k + b_k p(z_{t,l}|r_{l,k}, X_t);
    P̂(r̄_{l,k}|z_{t,l}, X_{1:t}, Z_{1:t-1}) = a_k + c_k;
  end for
end for
for all i map cells inside the FOV
  Obtain the set L_i of l_i measurement rays intersecting this cell
  if l_i > 0
    d = P(m_i|X_{1:t-1}, Z_{1:t-1}) ∏_{L_i} P̂(r_{l,k}|z_{t,l}, X_{1:t}, Z_{1:t-1});
    e = P(m̄_i|X_{1:t-1}, Z_{1:t-1}) ∏_{L_i} P̂(r̄_{l,k}|z_{t,l}, X_{1:t}, Z_{1:t-1});
    P(m_i|X_{1:t}, Z_{1:t}) = d/(d+e);
  else
    P(m_i|X_{1:t}, Z_{1:t}) = P(m_i|X_{1:t-1}, Z_{1:t-1});
  end if
  Return: P(m_i|X_{1:t}, Z_{1:t})
end for
```

TABLE I
FAST ALGORITHM OF THE EXACT SOLUTION OF THE INVERSE SENSOR MODEL FOR l SIMULTANEOUS MEASUREMENT RAYS

IV. NUMERICAL EXAMPLE

The purpose of this section is to compare the proposed exact solution to the inverse sensor model with an approximate algorithm developed for a Microsoft Kinect sensor [9], [12], summarized as follows. The probability that the i-th grid cell $\mathbf{m}_i$ is occupied conditioned on the measurement ray $z_{t,l}$ at the pose X_t is the continuous function

$$P(\mathbf{m}_i|z_{t,l}, X_t) = \begin{cases} 0.3 + (\frac{k}{\sigma\sqrt{2\pi}} + 0.2)e^{-\frac{1}{2}\left(\frac{\hat{z}_{l,i}-z_{t,l}}{\sigma}\right)^2} & \text{if } z_{t,l} \leq \hat{z}_{l,i}, \\ 0.5 + \frac{k}{\sigma\sqrt{2\pi}} e^{-\frac{1}{2}\left(\frac{\hat{z}_{l,i}-z_{t,l}}{\sigma}\right)^2} & \text{if } z_{t,l} > \hat{z}_{l,i}, \end{cases}$$

which is based on the expected distance to the cell $\hat{z}_{l,i}$ with parameters $k = \sigma = 0.6$. This follows the structure of the approximate inverse sensor model proposed in [8]. The main idea of this approach is that the probability of a cell being occupied (i) near a measurement is high (measurement likely hits this cell), (ii) between the robot and the measurement is

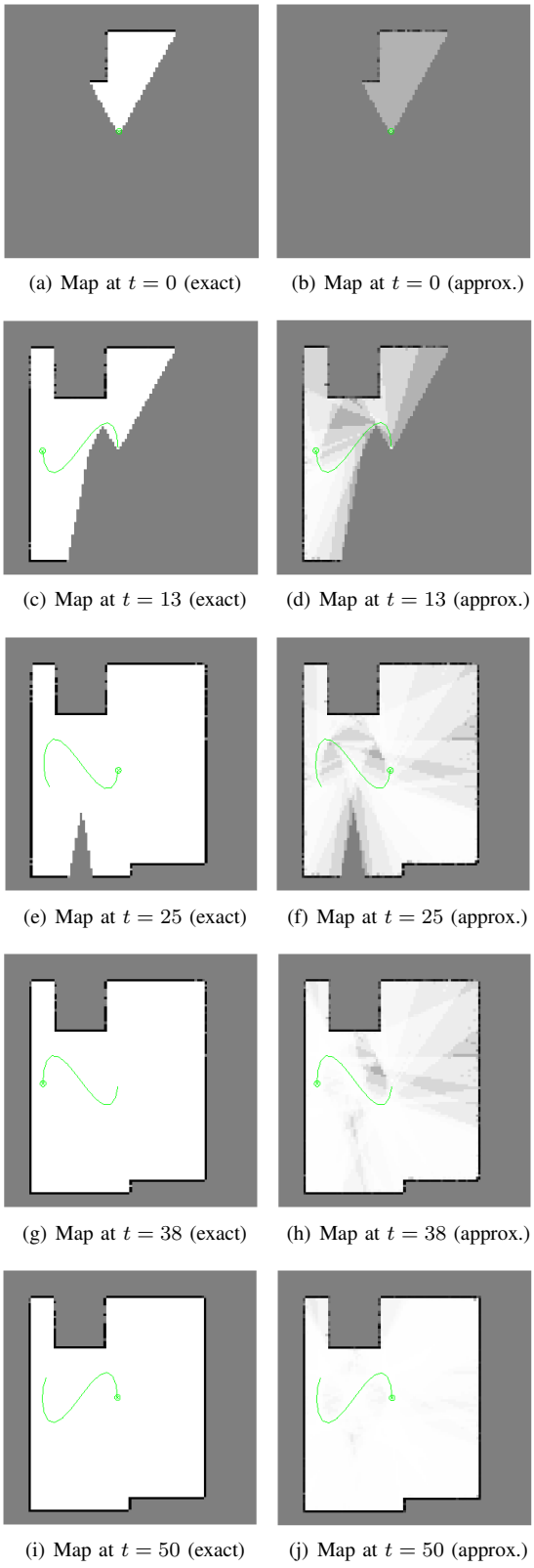

(a) Map at $t = 0$ (exact) (b) Map at $t = 0$ (approx.)

(c) Map at $t = 13$ (exact) (d) Map at $t = 13$ (approx.)

(e) Map at $t = 25$ (exact) (f) Map at $t = 25$ (approx.)

(g) Map at $t = 38$ (exact) (h) Map at $t = 38$ (approx.)

(i) Map at $t = 50$ (exact) (j) Map at $t = 50$ (approx.)

Fig. 1. A robot (green crossed circle, green curve of its previous 13 seconds) measures a room with a Kinect depth sensor. The exact inverse sensor model is compared with an approximate algorithm designed for the Kinect depth sensor. The algorithms update the grid cells from uncertain (grey, 0.5 occupancy probability) to either occupied (black, 1 occupancy probability) or free (white, 0 occupancy probability). Measured cells have occupancy probabilities closer to 0 or 1 as more information becomes available, and unmeasured cells remain near 0.5, or uncertain.

low (measurement passes through this cell), and (iii) beyond the measurement is unchanged (the robot cannot measure through a wall/object).

Then, these probabilities are combined in a weighted fashion such that all measurements rays of scan Z_t simultaneously update the same grid cell in a log-odds format,

$$\log\left(\frac{P(\mathbf{m}_i|Z_t, X_t)}{1 - P(\mathbf{m}_i|Z_t, X_t)}\right) = \frac{1}{\sum_{z_{t,l}\in\mathbf{m}_i} \hat{z}_{l,i}} \sum_{z_{t,l}\in\mathbf{m}_i} \log\left(\frac{P(\mathbf{m}_i|z_{t,l}, X_t)}{1 - P(\mathbf{m}_i|z_{t,l}, X_t)}\hat{z}_{l,i}\right).$$

A. Computation Time

The proposed ray inverse sensor model is designed to maintain the accuracy of the exact solution with substantial computational improvements. A 1-dimensional example is simulated on a Mac desktop computer with 11 grid cells, 10 of which are visible to the robot, where the same depth measurement is used for all occupancy grid algorithms. The computational time of the exact solution is computed in the conventional manner according to (5) in 2.3314 seconds to obtain the same solution of (6) from (7) and (8) in just 0.0027 seconds, which is 874.77 times faster. The approximate ray inverse sensor model completes in 0.0011 seconds, but this algorithm does not follow a forward sensor model, so the probabilities of the map may be inaccurate.

B. Trajectory Map Building

In this numerical example, we consider a robot in a two-dimensional environment composed of ten wall edges, and the robot follows a figure-eight curve, then turns around and completes the same curve in the reverse direction. The map is composed of 100×100 square grid cells with edge length of 1 cm. A forward sensor model $p(z_t|m, X_t)$ [4] is constructed according to the specifications of the Kinect sensor [12], and a pseudo-random measurement scan is sampled at each time step via the inverse transform sampling [13]. The same set of measurements updated each second are used with both occupancy grid mapping algorithms to construct the map.

The resulting maps are illustrated in Figure 1 for both algorithms, where it is shown that the proposed algorithm yields a substantially more accurate and clear map with less uncertainty. To quantify the degree of map uncertainty, we define the entropy of the map as

$$H(P(m|X_{1:t}, Z_{1:t})) = -\sum_{i=1}^{n} \big\{P(\mathbf{m}_i|X_{1:t}, Z_{1:t}) \log P(\mathbf{m}_i|X_{1:t}, Z_{1:t}) + (1 - P(\mathbf{m}_i|X_{1:t}, Z_{1:t})) \log(1 - P(\mathbf{m}_i|X_{1:t}, Z_{1:t}))\big\},$$

which is maximized when the probability of occupancy is 0.5 for all cells (more uncertain), and it is minimized when they are either 0 or 1 (less uncertain).

The change of the map entropy over time, and the entropy of the completed maps, for both methods are depicted in Figure 2. The subfigure (a) illustrates that the proposed exact inverse sensor model exhibits rapid decreases of entropies,

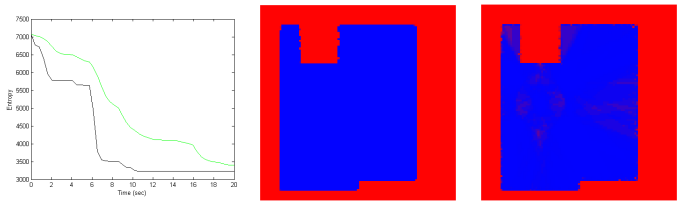

(a) Entropy change (b) $t = 50$ (exact) (c) $t = 50$ (approx.)

Fig. 2. Entropy serves as a measure of uncertainty of the occupancy grid, where more blue regions are more certain, and red regions are more uncertain. In (a), the entropy with the exact solution (black) decreases faster than the entropy with the approximate solution (green) over 20 seconds. The uncertainty is always less when the exact solution is applied, where the final map (50 seconds) with the approximate solution has more uncertainty.

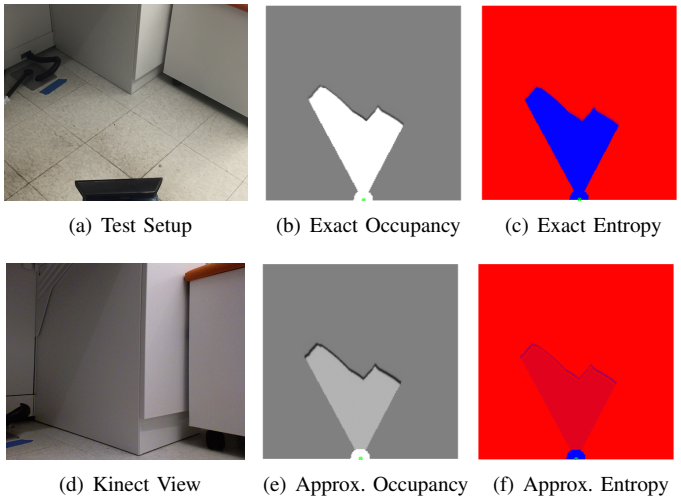

(a) Test Setup (b) Exact Occupancy (c) Exact Entropy

(d) Kinect View (e) Approx. Occupancy (f) Approx. Entropy

Fig. 3. The Kinect captures depth measurements of the underside of a metal desk. The measurement scan serves to update two occupancy grid mapping schemes. The proposed approach, based on the the exact solution of the inverse sensor model, provides an update with substantially less uncertainty than the approximate model update.

and smaller entropies always. The resulting terminal map obtained from the proposed approach, shown in the subfigure (b), has less uncertainty than (c) constructed by the approximate model. In short, the proposed approach is more efficient at extracting information about the environment from the same set of set measurements.

V. Preliminary Experimental Results

The proposed algorithm is also implemented to range measurements obtained from a Kinect sensor. The map is composed of 200×200 square grid cells with edge length of 1 cm. The parameters for the Kinect sensor are obtained from [12], and the OpenKinect library is used on a Mac computer to extract range measurements. The Kinect sensor faces walls underneath a work desk, as illustrated in Figures 3.(a) and (b). The resulting occupancy grid map and entropy map are obtained from both the proposed and approximate algorithms after a single scan [9], [12].

The proposed approach uses all the information from the measurement scans accurately. After the first scan, the free space has a substantially lower probability of occupancy. Furthermore, the edges of the objects captured by the Kinect are well defined with the proposed approach with an edge thickness of roughly one or two cells, but two or three cells thick with the conventional approach. Additionally, the decrease in entropy is greater with the proposed approach at -3487, compared with -557 with the approximate model.

VI. Conclusions

Occupancy grid mapping produces a probabilistic map of occupied space, but each probability is approximated in practice due to the perceived complications of the exact solution. This paper provides an exact solution to this complicated probability problem using cell occlusion in the forward sensor model. This yields a substantially simpler inverse sensor model, which avoids a potentially harmful Markov assumption that commonly appears in the log-odd ratio formations. The main contribution of this paper is that all of the information available in the measurements and the a priori estimate is extracted and integrated synergistically to generate a more accurate a posteriori map. The numerical and experimental results show that maps using this exact approach are substantially improved.

Appendix

A. Proof of Proposition 1

a) Unnormalized Reduced Map Inverse Sensor Model: For the reduced map of the l-th ray, the unnormalized probability corresponding to terms without $\eta_{t,l}$ in (5) is

$$\tilde{P}(\mathbf{r}_{l,k}|z_{t,l}, X_{1:t}, Z_{1:t-1}) = \sum_{r \in \mathcal{M}_k} p(z_{t,l}|r, X_t) P(r|X_{1:t-1}, Z_{1:t-1}). \quad (16)$$

Recall $\mathcal{M}_k$ corresponds to the set of maps where the k-th cell is occupied. Define a subset $\mathcal{N}_{i,k} \subset \mathcal{M}_k$ for $1 \leq i \leq k$ be the set of maps where the i-th cell is the first occupied cell. More explicitly,

$$\begin{aligned}\mathcal{N}_{i,k} &= \{r \in \mathcal{M}_k | \mathbf{r}_{l,i+}\} \\ &= \{r \in \mathcal{M}_k | \mathbf{r}_{l,1} = 0, \ldots, \mathbf{r}_{l,i-1} = 0, \mathbf{r}_{l,i} = 1, \mathbf{r}_{l,k} = 1\}.\end{aligned}$$

Then, $\mathcal{M}_k$ can be written as $\mathcal{M}_k = \bigcup_{i=1}^{k} \mathcal{N}_{i,k}$. Using this, the summation over $\mathcal{M}_k$ at (16) can be decomposed of the summation over each $\mathcal{N}_{i,k}$ to obtain

$$\tilde{P}(\mathbf{r}_{l,k}|z_{t,l}, X_{1:t}, Z_{1:t-1}) = \sum_{i=1}^{k} \left\{ \sum_{r \in \mathcal{N}_{i,k}} p(z_{t,l}|r, X_t) P(r|X_{1:t-1}, Z_{1:t-1}) \right\}.$$

This is motivated by the fact that the forward sensor model $p(z_{t,l}|r, X_t)$ is identical for all maps in $\mathcal{N}_{i,k}$, such that $p(z_{t,l}|r, X_t) = p(z_{t,l}|\mathbf{r}_{l,i+}, X_t)$ and it is moved left of the summation to obtain

$$\tilde{P}(\mathbf{r}_{l,k}|z_{t,l}, X_{1:t}, Z_{1:t-1}) = \sum_{i=1}^{k} \left\{ p(z_{t,l}|\mathbf{r}_{l,i+}, X_t) \sum_{r \in \mathcal{N}_{i,k}} P(r|X_{1:t-1}, Z_{1:t-1}) \right\}. \quad (17)$$

The last term of the above expression corresponds to the a priori probability of $\mathcal{N}_{i,k}$. When $i < k$, it is given by

$$\sum_{r\in\mathcal{N}_{i,k}} P(r|X_{1:t-1}, Z_{1:t-1}) = \left\{\prod_{j=0}^{i-1} P(\bar{\mathbf{r}}_{l,j}|X_{1:t-1}, Z_{1:t-1})\right\} \times P(\mathbf{r}_{l,i}|X_{1:t-1}, Z_{1:t-1}) P(\mathbf{r}_{l,k}|X_{1:t-1}, Z_{1:t-1}), \quad (18)$$

and when $i = k$,

$$\sum_{r\in\mathcal{N}_{k,k}} P(r|X_{1:t-1}, Z_{1:t-1}) = \left\{\prod_{j=0}^{k-1} P(\bar{\mathbf{r}}_{l,j}|X_{1:t-1}, Z_{1:t-1})\right\} \times P(\mathbf{r}_{l,k}|X_{1:t-1}, Z_{1:t-1}). \quad (19)$$

Substituting (18) and (19) into (17), we obtain (7).

b) Complement of the Unnormalized Reduced Map Inverse Sensor Model: An analytic expression for the complement of the unnormalized inverse sensor model is also required for obtaining the normalizer of the l-th ray at time t, namely $\eta_{t,l}$. Let $\bar{\mathcal{M}}_k$ be the set of maps where the k-th cell is unoccupied, i.e., $\bar{\mathcal{M}}_k = \{r \in \{0,1\}^{n_{r,l}} \,|\, \mathbf{r}_{l,k} = 0\}$. Similar to (16),

$$\tilde{P}(\bar{\mathbf{r}}_{l,k}|z_{t,l}, X_{1:t}, Z_{1:t-1}) = \sum_{r\in\bar{\mathcal{M}}_k} p(z_{t,l}|r, X_t) P(r|X_{1:t-1}, Z_{1:t-1}). \quad (20)$$

Let $\bar{\mathcal{N}}_{i,k} \subset \bar{\mathcal{M}}_k$ for $1 \le i \le n_{r,l}$ and $i \neq k$ be the set of maps where the i-th cell is the first occupied cell. More explicitly,

$$\bar{\mathcal{N}}_{i,k} = \{r \in \bar{\mathcal{M}}_k \,|\, \mathbf{r}_{l,1} = 0, \ldots, \mathbf{r}_{l,i-1} = 0, \mathbf{r}_{l,i} = 1, \mathbf{r}_{l,k} = 0\}.$$

Then, we have $\bar{\mathcal{M}}_k = \bigcup_{\substack{i=1\\ i\neq k}}^{n_{r,l}} \bar{\mathcal{N}}_{i,k}$. Note that the forward sensor model $p(z_{t,l}|r, X_t)$ is identical for any maps in $\bar{\mathcal{N}}_{i,k}$, such that $p(z_{t,l}|r, X_t) = p(z_{t,l}|\mathbf{r}_{l,i+}, X_t)$. Similar to (17),

$$\tilde{P}(\bar{\mathbf{r}}_{l,k}|z_{t,l}, X_{1:t}, Z_{1:t-1}) = \sum_{\substack{i=1\\ i\neq k}}^{n_{r,l}} \left\{ p(z_{t,l}|\mathbf{r}_{l,i+}, X_t) \sum_{r\in\bar{\mathcal{N}}_{i,k}} P(r|X_{1:t-1}, Z_{1:t-1}) \right\}, \quad (21)$$

where the last term corresponds to the a priori probability of $\bar{\mathcal{N}}_{i,k}$. When $i < k$, it is given by

$$\sum_{r\in\bar{\mathcal{N}}_{i,k}} P(r|X_{1:t-1}, Z_{1:t-1}) = \left\{\prod_{j=0}^{i-1} P(\bar{\mathbf{r}}_{l,j}|X_{1:t-1}, Z_{1:t-1})\right\} \times P(\mathbf{r}_{l,i}|X_{1:t-1}, Z_{1:t-1}) P(\bar{\mathbf{r}}_{l,k}|X_{1:t-1}, Z_{1:t-1}), \quad (22)$$

and when $k < i$,

$$\sum_{r\in\bar{\mathcal{N}}_{i,k}} P(r|X_{1:t-1}, Z_{1:t-1}) = \left\{\prod_{j=0}^{i-1} P(\bar{\mathbf{r}}_{l,j}|X_{1:t-1}, Z_{1:t-1})\right\} \times P(\mathbf{r}_{l,i}|X_{1:t-1}, Z_{1:t-1}). \quad (23)$$

Substituting (22) and (23) into (21), we obtain

$$\tilde{P}(\bar{\mathbf{r}}_k|z_{t,l}, X_{1:t}, Z_{1:t-1}) = P(\bar{\mathbf{r}}_{l,k}|X_{1:t-1}, Z_{1:t-1}) \times \left[\sum_{i=1}^{k-1} \left\{\prod_{j=0}^{i-1} P(\bar{\mathbf{r}}_{l,j}|X_{1:t-1}, Z_{1:t-1})\right\} \times p(z_{t,l}|\mathbf{r}_{l,i+}, X_t) P(\mathbf{r}_{l,i}|X_{1:t-1}, Z_{1:t-1})\right] + \left[\sum_{i=k+1}^{n_{r,l}+1} \left\{\prod_{j=0}^{i-1} P(\bar{\mathbf{r}}_{l,j}|X_{1:t-1}, Z_{1:t-1})\right\} \times p(z_{t,l}|\mathbf{r}_{i+}, X_t) P(\mathbf{r}_{l,i}|X_{1:t-1}, Z_{1:t-1})\right], \quad (24)$$

where $p(z_{t,l}|\mathbf{r}_{(n_r+1)+}, X_t)$ corresponds to the forward sensor model of maximum reading and $P(\mathbf{r}_{l,n_{r,l}+1}|X_{1:t-1}, Z_{1:t-1}) = 1$ for convenience for the empty map case.

c) Normalizer: We have

$$P(\mathbf{r}_{l,k}|z_{t,l}, X_{1:t}, Z_{1:t-1}) + P(\bar{\mathbf{r}}_{l,k}|z_{t,l}, X_{1:t}, Z_{1:t-1}) = 1.$$

Since they share the same normalizer $\eta_{t,l}$, this implies

$$\eta_{t,l} = \frac{1}{\tilde{P}(\mathbf{r}_{l,k}|z_{t,l}, X_{1:t}, Z_{1:t-1}) + \tilde{P}(\bar{\mathbf{r}}_{l,k}|z_{t,l}, X_{1:t}, Z_{1:t-1})}.$$

Substituting (7) and (24), and rearranging, we obtain (8).

REFERENCES

[1] D. Wolf and G. Sukhatme, "Mobile robot simultaneous localization and mapping in dynamic environments," *Autonomous Robots*, vol. 1, no. 19, pp. 53–65, 2005.

[2] K. Wurm, A. Hornung, M. Bennewitz, C. Stachniss, and W. Burgard, "Octomap: A probabilistic, flexible, and compact 3d map representation for robotic systems," in *Proceeding of the ICRA 2010 Workshop on Best Practice in 3D Perception and Modeling for Mobile Manipulation*, 2010.

[3] M. Montemerlo, S. Thrun, D. Koller, and B. Wegbreit, "Fastslam: A factored solution to the simultaneous localization and mapping problem," in *Proceeding of the National Conference on Artificial Intelligence (AAAI)*, Edmonton, Canada, 2002, pp. 593–598.

[4] S. Thrun, W. Burgard, and D. Fox, *Probabilistic Robotics*, ser. Intelligent Robotics and Autonomous Agents. Cambridge, Massachusetts: Massachusetts Institute of Technology, 2005.

[5] H. P. Moravec and A. Elfes, "High resolution maps from wide angle sonar," in *IEEE Conference on Robotics and Automation*, 1985.

[6] A. Elfes, "Using occupancy grids for mobile robot perception and navigation," *IEEE Computer*, pp. 46–57, 1989.

[7] H. Choset, K. Lynch, S. Hutchinson, G. Kantor, W. Burgard, L. Kavraki, and S. Thrun, *Principles of Robot Motion: Theory, Algorithms, and Implementations*, ser. Intelligent Robotics and Autonomous Agents. Cambridge, Massachusetts: Massachusetts Institute of Technology, 2005.

[8] F. Adert, "Drawing stereo disparity images into occupancy grids: Measurement model and fast implementation," in *Proceedings of the 2009 IEEE/RSJ International Conference on Intelligent Robots and Systems*, 2009.

[9] K. Pirker, M. Ruther, H. Bischof, and G. Schweighofer, "Fast and accurate environment modeling using three-dimensional occupancy grids," in *Proceedings of the 2011 IEEE International Conference on Computer Vision Workshops*, 2011.

[10] S. Thrun, "Learning occupancy grids with forward models," in *Proceedings of the 2001 IEEE/RSU International Conference on Intelligent Robots and Systems*, 2001.

[11] ——, "Learning occupancy grid maps with forward sensor models," *Autonomous Robots*, vol. 15, no. 2, pp. 111–127, 2003.

[12] K. Khoshelham and S. O. Elberink, "Accuracy and resolution of kinect depth data for indoor mapping applications," *Sensors*, pp. 1437–1454, 2012.

[13] L. Devroye, *Non-Uniform Random Variate Generation*. New York: Springer-Verlag, 1986.